Chempublish Journal
Journal Homepage: online-journal.unja.ac.id/chp
Department of Chemistry
Faculty of Science and Technology
Universitas Jambi
ISSN (Online): ISSN 2503-4588
No. 23/E/KPT/2019

Article

Designing L-type Amino Acid Transporter 1-targeting Cancer Theranostic Radiopharmaceuticals: A Molecular Docking Simulation

Holis Abdul Holik[1*], Arifudin Achmad[2], Faisal Maulana Ibrahim[1], Angela Alysia Elaine[1], Jonathan Stefanus[1], B.S. Ari Sudarmanto[3], Achmad Hussein S. Kartamihardja[2]

[1]*Department of Pharmaceutical Analysis & Medicinal Chemistry, Faculty of Pharmacy, Universitas Padjadjaran; Hegarmanah, Jatinangor, Sumedang 45363, West Java, Indonesia*

[2]*Department of Nuclear Medicine and Molecular Theranostics, Faculty of Medicine, Universitas Padjadjaran, Bandung 40162, West Java, Indonesia*

[3]*Laboratory of Medicinal Chemistry, Department of Pharmaceutical Chemistry, Faculty of Pharmacy, Universitas Gadjah Mada, D.I. Yogyakarta 55281, Indonesia*

Abstract

L-type amino acid transporter 1 (LAT1) is a potential pan-cancer theranostic molecular target. The LAT1 inhibitory potencies of eight theranostic radiopharmaceuticals designed based on a potent LAT1 inhibitor ADPB (in vitro predicted pIC_{50} 6.19), were estimated in molecular docking simulations. The designs comprised ADPB as a carrier molecule with/without 6-aminohexanoic acid (Ahx) linker, a chelating agent, and a radiometal (68Ga or 177Lu). JPH203, the most potent LAT1 inhibitor (predicted pIC_{50} 7.22), was utilized as a benchmark compound. A set of known LAT1 ligands (n = 15) were first docked into LAT1 to build the docking protocol with the software Molecular Operating Environment (MOE). Adding a linker improved the LAT1 inhibitory potency of DOTA-conjugated and NODAGA-conjugated ADPB-based theranostic radiopharmaceutical designs. 177Lu-DOTA-Ahx-ADPB has the exceptional LAT1 inhibitory potency (predicted pIC_{50} 51.55 ± 17.06) while 177Lu-DOTA-ADPB, its non-linker counterpart, has LAT1 inhibitory potency significantly higher than the native JPH203. The evaluation of docking poses and quantitative analysis for both 177Lu-DOTA-Ahx-ADPB and 177Lu-DOTA-ADPB have strong bonds with key amino acids on the LAT1 binding pocket, particularly Asn258, Tyr259, and the gating residue Phe252. Our findings provide a quantitative and illustrative understanding of the LAT1 inhibitory potency of LAT1-targeting theranostic radiopharmaceutical designs relevant to the rational design of pan-cancer radiotheranostic drugs.

Keywords: *Chelating agent, LAT1, pan-cancer, Molecular Operating Environment (MOE), theranostic radiopharmaceutical,*

* **Corresponding author**
Email addresses: holis@unpad.ac.id

DOI: https://doi.org/10.22437/chp.v9i2.44633
Received August 28th 2025; **Accepted** October 07th 2025; **Available online** December 31st 2025

Graphical Abstract

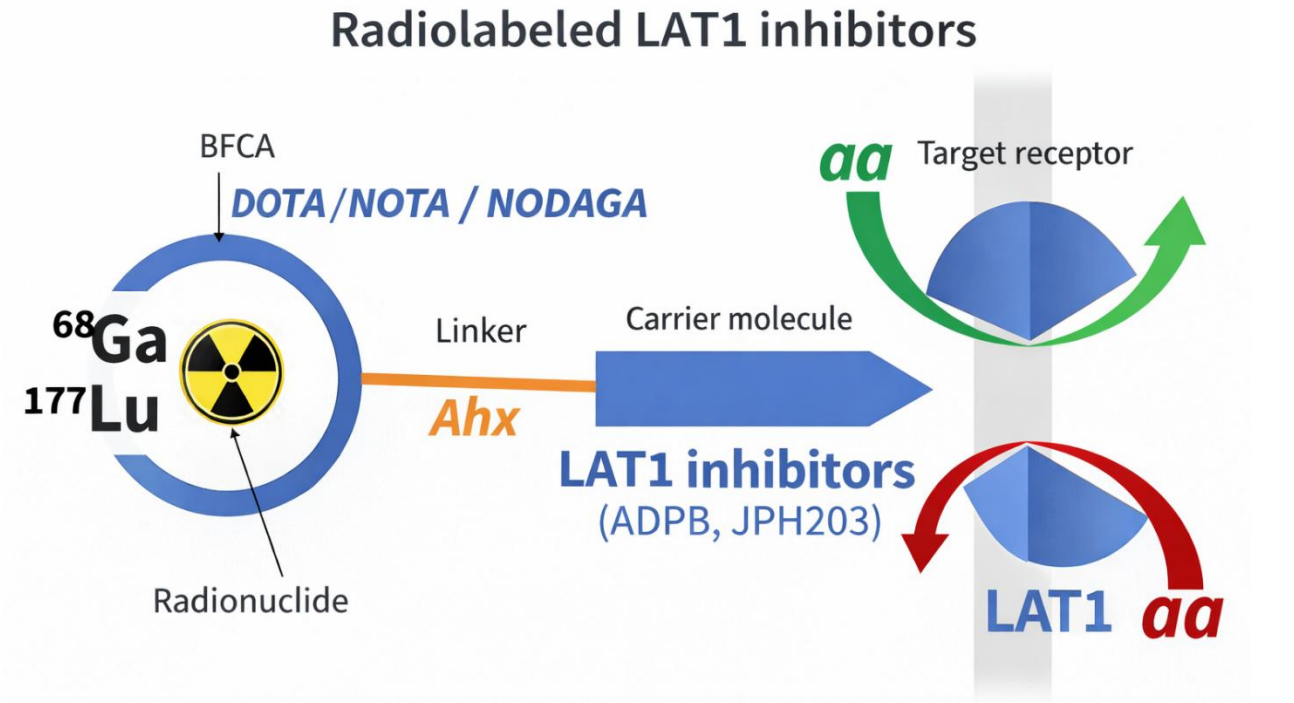

Introduction

The global burden of cancer is expected to be 28.4 million cases in 2040, equal to a 47% rise from the current figures [1]. Thus, earlier tumor entity characterization and metastasis detection are increasingly important for accurate staging and personalized cancer therapy. Systematic integration of diagnostic nuclear imaging and targeted nuclear therapy using a single molecular-targeting compound (termed "radiotheranostics") is now commenced thanks to the validation of molecular cancer targets (e.g., prostate-specific membrane antigen (PSMA), somatostatin receptors (SSTRs)) and the rapid development of advanced chemical scaffolds for radiopharmaceuticals (cancer-specific carrier molecules, radiometals, chelating agents, and pharmacokinetic-modifying linkers). In addition, successful clinical translation has been shown in advanced prostate cancer and gastrointestinal neuroendocrine malignancies [2,3]. Recently, fibroblast activation protein (FAP) and C-X-C motif chemokine receptor 4 (CXCR4) were considered potential pan-cancer targets, and theranostic radiopharmaceuticals developed accordingly demonstrated promising preliminary clinical translation (e.g., ^{68}Ga-FAPI-04, ^{68}Ga-pentixafor). However, several inherent challenges remain, as FAP-targeting might be less reliable in non-desmoplastic tumors [4], while CXCR4-targeting might be less useful in several solid tumors than in hematologic malignancies [5].

L-type amino acid transporter 1 (LAT1), a Na^+-independent bidirectional amino acid transporter with broad substrate specificity toward large neutral hydrophobic/aromatic amino acids and other substrates such as L-DOPA, melphalan, and gabapentin, has long been proven influential in cancer proliferation [6]. Furthermore, recent evidence validates that LAT1 satisfies the requirements as a pan-cancer target for being: 1) consistently overexpressed in the plasma membrane of all types of cancer cells, 2) limited expressed in normal cells

[7,8], and 3) instrumental in promoting multiple cancer hallmarks [9]. L-[3-^{18}F]-α-methyltyrosine (**^{18}F-FAMT**), a LAT1-specific PET probe, has been demonstrated to be cancer-specific and able to discriminate malignant lesions from non-cancerous lesions, including inflammation [10,11]. The low background uptake in ^{18}F-FAMT PET images also confirmed the lacking expression of LAT1 in normal tissues [7]. Until recently, several "LAT1-specific" radiopharmaceuticals have been developed (e.g., ^{18}F-FAMT , L-[2-^{18}F]-α-methylphenylalanine (**^{18}F-FAMP**) [12], (S)-2-amino-3-[3-(2-^{18}F-fluoroethoxy)-4-iodophenyl]-2-methylpropanoic acid (**^{18}F-FIMP**) [13], 4-borono-2-[^{18}F]-fluoro-L-phenylalanine (**^{18}F-FBPA**) [14], 2-[^{18}F]-2-fluoroethyl-L-phenylalanine (**^{18}F-FELP**) [15] and **^{18}F-NKO-035** [16,17]. However, even though some among them showed clinical potential, none were genuinely designed as a theranostic radiopharmaceutical. Therefore, the design of new compounds is needed to develop and apply theranostic radiopharmaceuticals for clinical use in cancer patients.

(S)-2-amino-4-(3,5-dichlorophenyl)butanoic acid (ADPB, predicted pIC_{50} 6.19) and S-(3-bromo-4-methoxybenzyl)-L-cysteine (predicted pIC_{50} 4.48) are two potent LAT1 inhibitors revealed through dynamic pharmacophore-based screening of libraries containing 1.1 million small molecules [18]. ADPB has several properties suitable to be developed as LAT1-targeting theranostic radiopharmaceuticals, i.e., 1) a simple and similar structure to L-phenylalanine (a system-L substrate and the most commonly used compound to evaluate LAT1 transport activity), 2) possession of halogen atoms on its hydrophobic side chain similar to LAT1 non-transportable blockers (e.g., triiodothyronine (T3) and tetraiodothyronine (T4)) [19], and 3) conjugation possibility with a chelating agent or a pharmacokinetic-modifying linker via a simple 1-ethyl-3-(3-dimethylaminopropyl)carbodiimide (**EDC**) and N-hydroxysulfosuccinimide (**NHS**) ester coupling chemistry (**Figure 1**) [20]. Furthermore, the recent availability of a high-resolution human LAT1 crystal structure in an outward-facing conformation opens the possibility of screening new inhibitors [21].

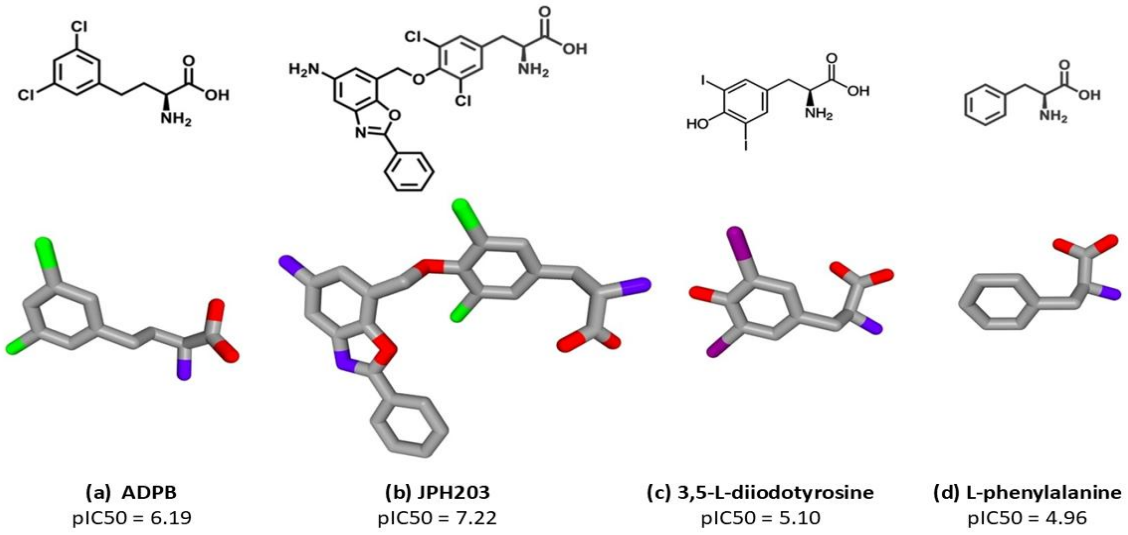

Figure 1. The chemical structure of LAT1 inhibitors (a) ADPB; (b) JPH203; (c) and 3,5-L-diiodotyrosine/Diiodo-Tyr) and (d) LAT1 substrate (L-phenylalanine).

In this study, LAT1-targeting theranostic radiopharmaceutical scaffold was designed as follows: ADPB as the carrier molecule; a hydrophobic, flexible linker 6-aminohexanoic acid (Ahx) [22]; bifunctional chelating agents (1,4,7,10-tetraazacyclododecane-1,4,7,10-tetraacetic acid (DOTA) or 1,4,7-triazacyclononane-1,4,7-triacetic acid (NOTA) or 1,4,7-triazacyclononane,1-glutaric acid-4,7-acetic acid (NODAGA)), and theranostic pair radiometals (^{68}Ga or ^{177}Lu) [23]. A substantial modification in the chemical structure of the carrier molecule, especially the addition of a radiometal-chelator complex and linker/spacer, might drastically change the binding affinity of an inhibitor. Therefore, the current molecular docking simulations aim to evaluate the LAT1 inhibitory potency of ADPB-based theranostic radiopharmaceuticals. **JPH203** (Nanvuranlat, (S)-2-amino-3-(4-((5-amino-2-phenylbenzo[D]oxazol-7-yl)methoxy)-3,5-dichlorophenyl)propanoic acid), the most potent LAT1 inhibitor (predicted pIC_{50} = 7.22) [24], was utilized as a comparison and the benchmark for LAT1 inhibitory potency.

Materials And Methods

The workflow of our molecular docking simulations is illustrated in **Supp. Data S1.**

Computational Study Software

Softwares used in this computational study are MarvinSketch (MarvinSuite Europium 7 (19.21.7) ChemAxon, https://www.chemaxon.com) for build 2D structure of ligands and Molecular Operating Environment v2020.09 (**MOE**) software (Chemical Computing Group, Montreal, QC, Canada) for build 3D structure of ligands and semi-empirically optimize the ligands.

Preparation of Radiopharmaceutical Ligands for Computational Study.

The general schematic design of theranostic radiopharmaceutical compounds for computational study are illustrated in **Figure 2**. The compounds were designed with the following components: a carrier molecule (ADPB or JPH203), a chelator (DOTA, NOTA, and NODAGA), and a radiometal (^{68}Ga or ^{177}Lu). All designs were built with or without a pharmacokinetic-modifying linker (6-aminohexanoic acid (Ahx)). The amine group of the carrier molecule was modified to form an amide bond with a carboxylate group of chelator or linker to allow conjugation via simple EDC– N-hydroxysulfosuccinimide ester chemistry later in the experimental synthesis. Of note, JPH203 has two free amide groups; thus, conjugation with a chelating agent generates three different conjugates (JPH203_x, JPH203_y, and JPH203_z; see Supp. Data S2). Representative 2D and 3D designs were illustrated in Supp. Data S2. All three chelators are compatible with ^{68}Ga radiolabeling, while ^{177}Lu radiolabeling was only evaluated in DOTA-conjugated designs. A complete list of all theranostic radiopharmaceutical designs is in Supp. Data S3.

Preparation of Target Molecule

The heterodimer complex of the human LAT1-subunit 4F2hc was downloaded from the Protein Data Bank of the Research Collaboration for Structural Bioinformatics website (www.rcsb.org, PDB ID: 7DSQ). The 3D complex structure of human LAT1, newly solved from cryo-electron microscopy images (resolution 3.4 Å), is in an outward-facing conformation with 3,5-L-diiodotyrosine (Diiodo-Tyr, predicted pIC_{50} = 5.10) as a native substrate bound on its substrate binding pocket [21]. Before

preparation, Diiodo-Tyr was removed from the LAT1 substrate binding pocket. Then, the preparation of the LAT1 was performed using the QuickPrep functionality in MOE. During this process, protonation states were determined, missing hydrogen atoms were added, missing amino acid sequences were modeled, and the resulting complex structure was energetically minimized. The side chain of amino acid residues in the LAT1 binding pocket was made flexible, while the main chain remained rigid. Water molecules were removed from the LAT1 complex after the preparation step.

Validation of Docking Pose

To validate that the binding pocket did not experience a significant change after the preparation, pose validation was performed by redocking Diiodo-Tyr into the post-prepared LAT1 in several simulations using multiple parameters. The docking poses of Diiodo-Tyr in the post-prepared LAT1 binding pocket were superposed against its original pose. The root-mean-square distance (RMSD) < 2 Å difference between the most rational post-preparation pose and the original pose was considered no significant departure.

***Refinement Trial*.**

MOE software package allows one to choose one of five scoring functions available (London dG, ASE, Affinity dG, Alpha HB, and GBVI/WSA dG) to approximate the binding affinity (Gibbs free energy, ΔG, unit: kcal/mol) between two molecules after they have been docked (algorithm of each scoring function is explained in **Supp. Data S4**). Trial docking was performed to approximate the quantitative docking results closer to the actual LAT1 inhibition using known LAT1 ligands retrieved from the literature. Known LAT1 ligands (n = 15, including JPH203 and phenylalanine, **Supp. Data S5**) were each docked into the 3D structure of LAT1 using all five scoring functions. First, docking scores (S, unit: kcal/mol) of each known LAT1 ligand were plotted in a linear Pearson correlation analysis toward their corresponding predicted pIC_{50} values. Then, the scoring function producing the best correlation coefficient (R^2) between these two variables was selected for the subsequent docking simulations. The corresponding linear regression formula (predicted pIC_{50} = a(S) + b) was eventually used to estimate the LAT1 inhibitory potency of each theranostic radiopharmaceutical design.

The data of known LAT1 ligands were obtained from the ChEMBL database (www.ebi.ac.uk/chembl/), including the detailed 2D structure and predicted pIC_{50} against LAT1 from previously published in vitro or in vivo experiments. In addition, an identical preparation method was applied to these known LAT1 ligands. Trial docking also generated a LAT1 inhibition pharmacophore to which the 3D docking pose will be evaluated.

Docking Protocol*, *Docking Pose Evaluation, and Quantitative Analysis

The docking protocol was generated by varying the configuration for defining the binding site, the presence of crystallographic waters for hydrogen-bond mediation (WC), ligand and receptor protonation states (ph4), and the pose placement algorithm (placement) in MOE. The results of the docking protocol variations were then calculated using root-mean-square deviation (RMSD), and the protocol with the lowest RMSD was selected. Molecular docking simulations of theranostic radiopharmaceutical designs' binding to LAT1 were performed using the triangle method as a placement method with a timeout of 300 s, London dG scoring function

in 1,000 iterations, and the exploration for best conformation was repeated 30 times. Force field was used as a refinement method by applying MMFF94x. The best conformations of each theranostic radiopharmaceutical design were chosen for further analysis. The criteria used were based on their more negative S values, most rational poses (carrier molecule inside the binding pocket), and best intermolecular interactions with key amino acid sequences on the LAT1 binding pocket.

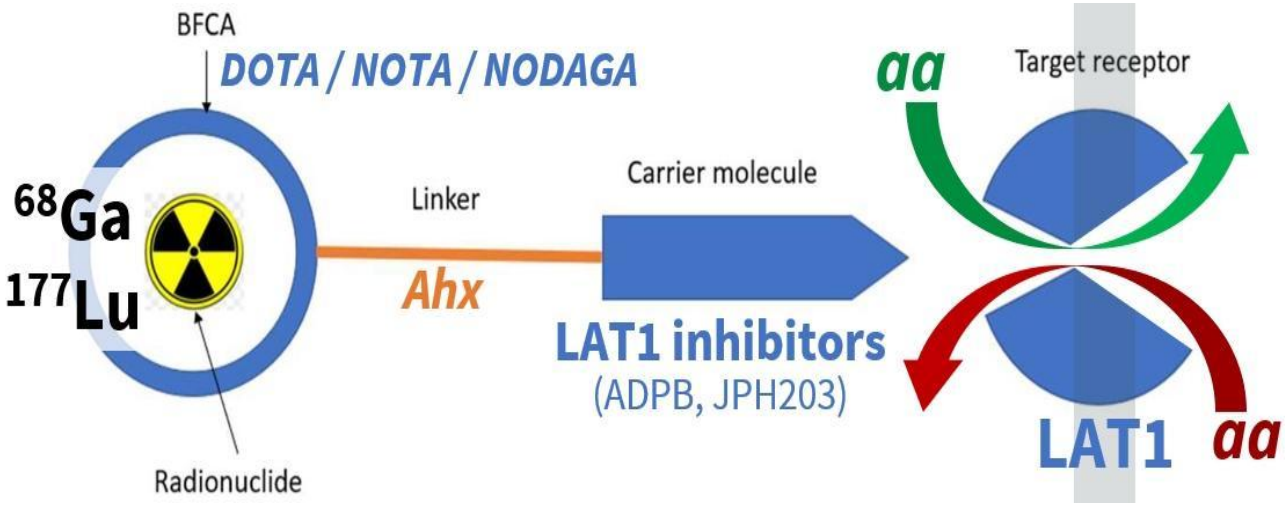

Figure 2. Schematic figure of theranostic radiopharmaceutical designs. (Notes: aa = amino acids, BFCA = bifunctional chelating agent.

Evaluation of the Docking Poses and Quantitative Analyses

LAT1 inhibitory potency (estimated predicted pIC_{50}) of ADPB-based and JPH203-based theranostic radiopharmaceuticals (predicted pIC_{50}) was compared accordingly (based on their radiometal and linker). The in vitro predicted pIC_{50} of native ADPB (6.19) and native JPH203 (7.22) was set as the lower limit in finding which theranostic radiopharmaceutical design has better LAT1 inhibition potential [19]. Statistical analyses were made to compare the central tendency values (mean or median) of the two unpaired groups (Students' *t* or Mann-Whitney U test, where applicable). The statistical significance level was $p < 0.05$ (95% confidence interval). Statistical analysis was performed using GraphPad Prism software (version 6, GraphPad Software, La Jolla CA, USA. www.graphpad.com).

The intermolecular interactions of key amino acid residues on LAT1 binding pocket with each theranostic radiopharmaceutical design in its particular pose were visualized and analyzed in 2D using Biovia Discovery Studio 2016 (Biovia Dassault Systèmes, San Diego, US) and in 3D using MOE. Those key amino acid residues are Phe252 (F252, a gating element), Trp257 (W257), Tyr259 (Y259), and ASN258 (N258) [25]. The docking poses in MOE were also used to confirm LAT1 inhibition pharmacophore occupancy of each pose and predict the linker's role toward the conformity of each theranostic radiopharmaceutical design. The .pdb files obtained were reconstructed for further 3D visualization using Biovia Discovery Studio 2016.

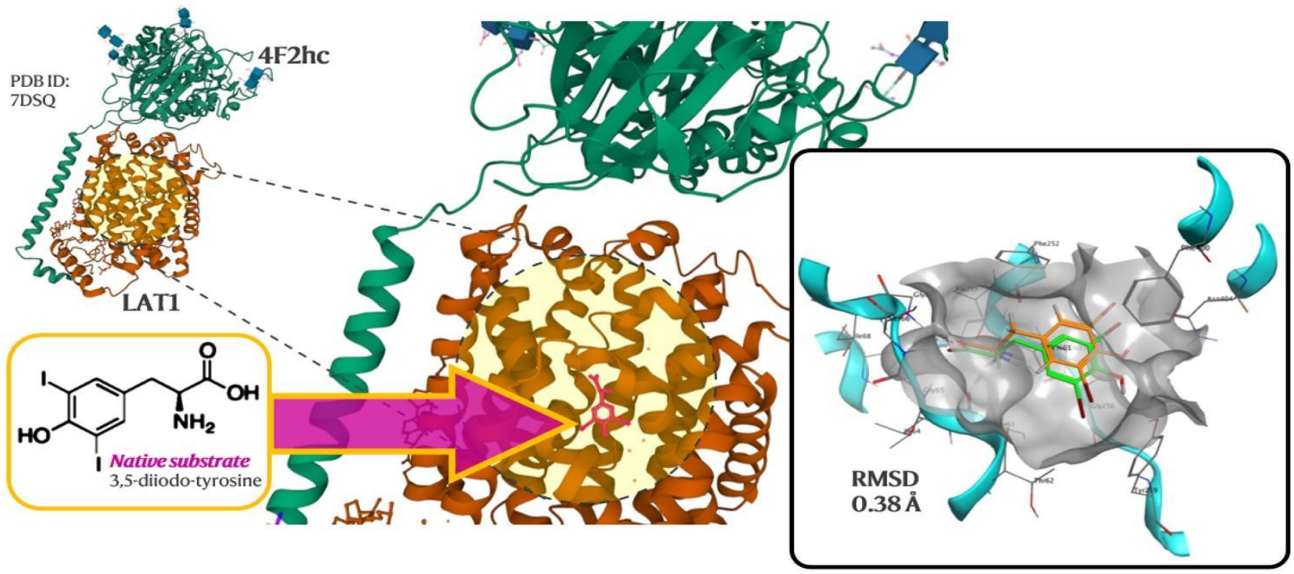

Figure 3. The 3D structure of human LAT1 with Diiodo-Tyr occluded the LAT1 substrate binding pocket. Overlaid image (box) of Diiodo-Tyr docking pose post-preparation (*orange*) and its original pose (*light green*) during pose validation

Evaluation of the Docking Poses and Quantitative Analyses

LAT1 Inhibitory Potency of ADPB-based Theranostic Radiopharmaceutical Design. All theranostic radiopharmaceutical designs in this study demonstrated negative docking scores (Supp. Data S3). Generally, ADPB-based theranostic radiopharmaceutical designs did not exhibit a higher LAT1 inhibitory potency than the JPH203-based ones (Supp. Data S7). ^{177}Lu-DOTA-Ahx-ADPB, ^{177}Lu-DOTA-ADPB, and ^{68}Ga-NODAGA-Ahx-ADPB were the only three among eight ADPB-based theranostic radiopharmaceutical designs having a LAT1 inhibitory potency better than their native form (ADPB). However, based on statistical comparison of LAT1 inhibitory potencies among ADPB-based theranostic radiopharmaceutical, native ADPB, and native JPH203, ^{177}Lu-DOTA-Ahx-ADPB and ^{177}Lu-DOTA-ADPB demonstrated LAT1 inhibitory potency significantly higher than native JPH203 (P value = 0.0044 for ^{177}Lu-DOTA-Ahx-ADPB and P value = 0.00227 for ^{177}Lu-DOTA-ADPB) (Figure 4, Supp. Data S8). ADPB-based and JPH203-based theranostic radiopharmaceutical designs containing ^{177}Lu radiometal demonstrated a higher LAT1 inhibitory potency than those with ^{68}Ga radiometal based on predicted pIC_{50} value (**Supp.Data S3**). ADPB-based and JPH203-based radiopharmaceuticals with the radiometal ^{177}Lu have estimated predicted pIC_{50} values in the range of 51.57 to 87.12, while APBD-based and JPH203-based radiopharmaceuticals with the radiometal ^{68}Ga have estimated predicted pIC_{50} values in the range of 1.96 to 17.48. In addition, adding an Ahx linker improves LAT1 inhibitory potency of ADPB-based designs, except if a NOTA chelator was used (**Figure 4**). However, such improvement was not observable in JPH203-based designs (**Supp. Data S7**). Therefore, to analyze further the extraordinary LAT1 inhibitory potency of ^{177}Lu-DOTA-Ahx-ADPB and ^{177}Lu-DOTA-ADPB, subsequent analyses involved ^{68}Ga-DOTA-Ahx-ADPB and ^{68}Ga-DOTA-ADPB.

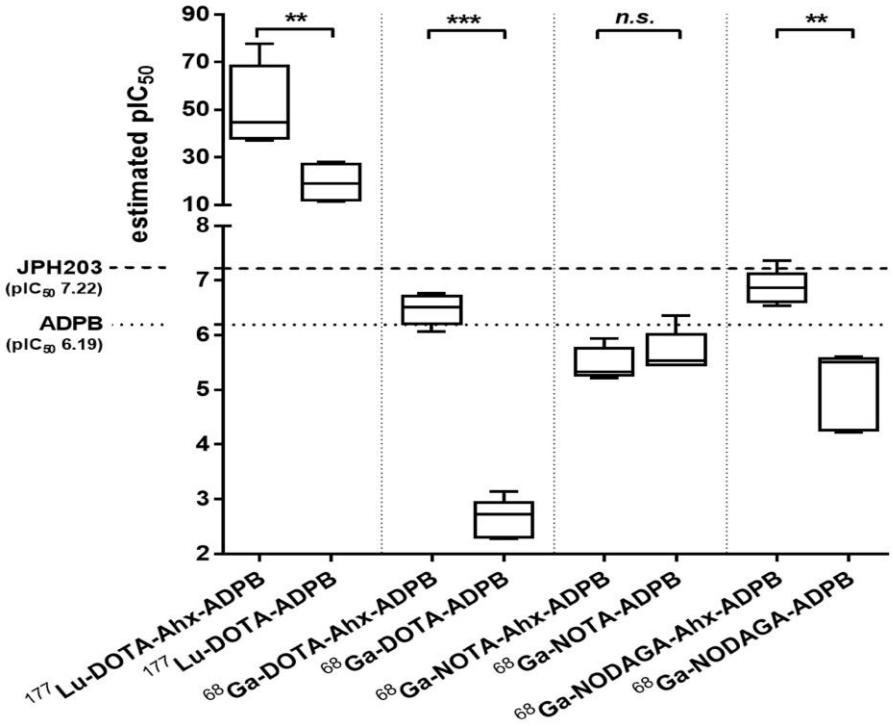

Figure 4. Estimated predicted pIC_{50} of ADPB-based theranostic radiopharmaceutical designs; n = 5 for each design, **n.s.** statistically not significant, ****** p <0.001, ******* p <0.0001.

Intermolecular interactions with amino acids residue in LAT1 substrate binding pocket

^{177}Lu-DOTA-Ahx-ADPB and ^{177}Lu-DOTA-ADPB have hydrogen bonds with key amino acid residues on the LAT1 binding pocket, particularly Asn258, Tyr259, and the gating residue Phe252. ^{68}Ga-DOTA-Ahx-ADPB and ^{68}Ga-DOTA-ADPB, on the other hand, lack strong intermolecular interactions based on the hydrogen bond formed between LAT1 and these compounds as ligands (**Table 1**, **Figure 5**). The 3D docking poses and detailed interactions are provided in **Figure 6**, **Figure 7**, and mol2 3D molecular model files in **Additional Files**.

LAT1 has been reported overexpressed on the cancer cell membranes in all malignancies and prognostic for poor clinical outcomes [26,27]. The LAT1 expression, however, has been confirmed limited in normal tissue [7]. Therefore, LAT1 is a promising *pan-cancer* radiotheranostic target. In this work, we proposed theranostic radiopharmaceutical designs based on a LAT1 inhibitor ADPB and computed its LAT1 inhibitory potentials through molecular docking simulations. The selection basis of ADPB as the carrier molecule was multiple. First, ADPB (predicted pIC_{50} = 6.19) has been validated experimentally as a potent LAT1 inhibitor with an inhibition potential higher than natural LAT1 substrates (essential amino acids, neutral amino acids with large side chains, e.g.: Leu, Val, Ile, Phe, Trp, His, Met, Tyr). The ADPB structure is similar to L-phenylalanine, the most widely used LAT1 natural substrate in the LAT1 transport evaluation and structure-based discovery for LAT1 inhibitors [18]. The other reason is that ADPB possesses two halogen atoms, similar to JPH203, the most potent LAT1 inhibitor, and other high-affinity LAT1 ligands (e.g., T3, T4, Diiodo-Tyr) (**Figure 1**).

Table 1. Intermolecular interaction between ADPB-based theranostic radiopharmaceuticals and key amino acids residues in the LAT1 substrate binding pocket

ADPB-based theranostic radiopharmaceutical designs	**Estimated predicted pIC_{50}** (±SD)	**1** **Conventional Hydrogen Bond**	**2** **Other interactions**	**3** **Carbon Hydrogen Bond**	**4** **π–π interactions**	**5** **Van der Waals force**	**6** **π-Alkyl interaction**
^{177}Lu-DOTA-Ahx-ADPB	**51.55** ±17.06	**ASN258**, ARG141, ASN404	**TRP257** (Pi-Sigma)	**PHE252**, **ASN258**, **TYR259**, ASP116, GLU136, SER401	**–**	PHE403, CYS407, PHE262, LYS132, VAL408, LEU349, LEU251, ILE397, THR62, SER338, VAL148, ***GLY65***, ***SER66***, ***GLY67***, TYR264, SER96, SER144, TRP405, GLY255, ***PHE400***, GLY256	**PHE252**, VAL148, ILE147, ***PHE400***
^{177}Lu-DOTA-ADPB	**19.42** ±7.58	**ASN258**, ASN404	**–**	GLY256, **TYR259**, GLY255, ASP116,	**–**	**TRP257**, ARG141, ILE140, ILE397, ***SER66***, ***GLY65***, ILE63, ***GLY67***, SER144, THR62, PHE403, PHE262, SER342, LYS132, CYS407, VAL408	**PHE252**, VAL148, ILE147, ***PHE400***,
^{68}Ga-DOTA-Ahx-ADPB	**6.47** ±0.27	THR62	**–**	***GLY65***	***PHE400***	**PHE252**, **ASN258**, VAL70, ILE397, THR71, VAL151, PHE394, VAL148, ASN404, GLY256, SER144, GLY255, SER338, ILE63, ILE147, ***GLY67***	**TYR259**
^{68}Ga-DOTA-ADPB	**2.64** ±0.35	***SER66***, ILE63	**–**	THR71, ***GLY65***, ***GLY67***, GLY256 (Pi-donor)	**TRP257**, GLY255, TRP405	**PHE252**, **ASN258**, GLY74, VAL70, ILE64, THR62, SER338, VAL148, **TYR259**, LEU251, ILE147, VAL408, ***PHE400***, ALA253, VAL151, ILE397, LYS453, PHE394, SER249	–

Note: Key amino acid residues were typed in **bold**. Amino acid residues typed in ***bold-italic*** were also mentioned in literature as important gating components. Numbers in the first row indicate the interaction strength from high to low.

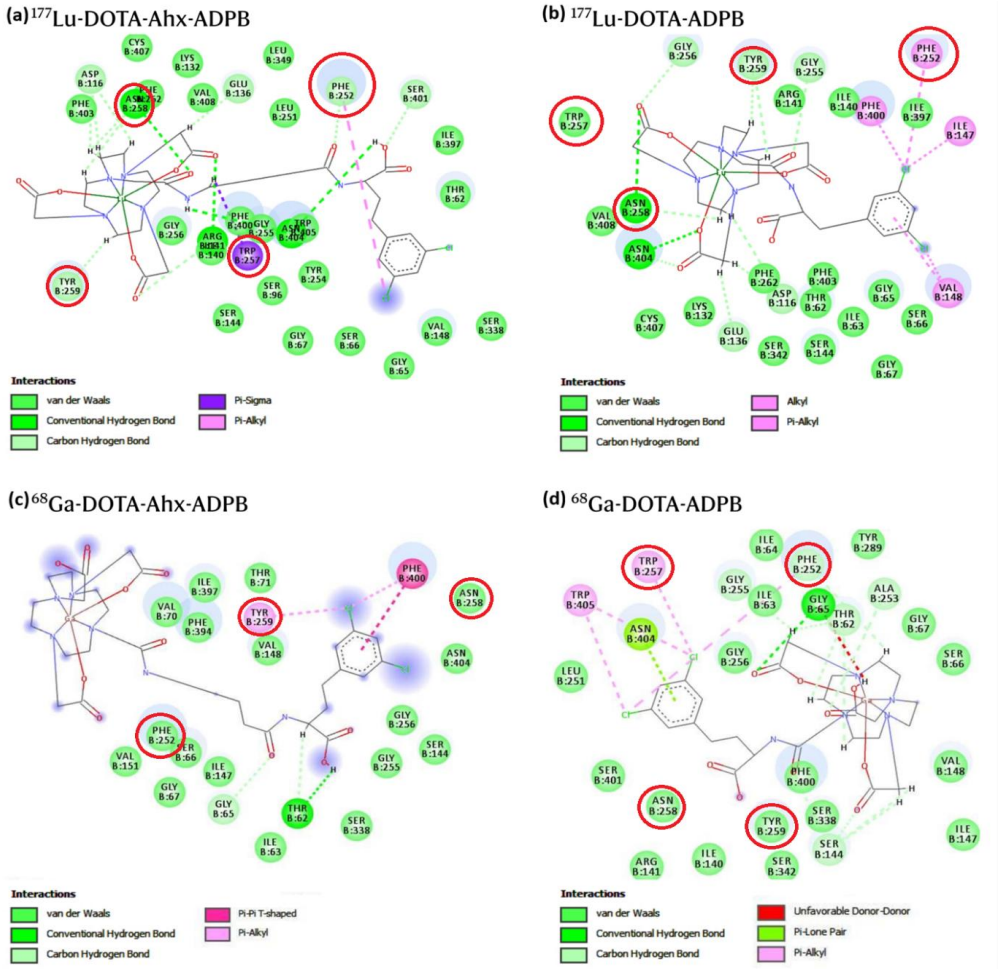

Figure 5. Intermolecular interaction between ADPB-based theranostic radiopharmaceuticals and key amino acids residues in the LAT1 substrate binding pocket. Key amino acid residues were mark with red circle.

The non-covalent interaction of halogen atoms has been experimentally proven essential in LAT1 ligand recognition and in making polar contacts with the amino acid side chains, especially for small molecules like ADPB [19]. Despite relatively smaller and more simple, ADPB retains LAT1 inhibitory potency comparable to other potential LAT1 inhibitors, e.g., JX-078 (predicted pIC_{50} = 6.92), JX-075 (predicted pIC_{50} = 6.78), JX-119 (predicted pIC_{50} = 6.23)[7], and SKN103 (predicted pIC_{50} = 5.70) [28].

JPH203 (KYT0353), the most potent LAT1 inhibitor (predicted pIC_{50} 7.22) to date, has been evaluated using in vitro and in vivo models of various cancers and is currently being challenged in phase II clinical trial for cholangiocarcinoma [24]. Even though JPH203 was cleverly designed to be structurally fit within the LAT1 binding pocket, unfortunately, its large side chain with multiple rings renders it rigid and large, thus leaving no room for additional chemical scaffold required for theranostic moieties. On the other hand, ADPB is still considerably smaller than JPH203, even though it possesses an extra carbon length compared to L-phenylalanine and Diiodo-Tyr. This feature allows ADPB to satisfy the LAT1 inhibition pharmacophore while providing enough space for additional chemical scaffolds [18]. Furthermore, ADPB has a single primary amine capable of conjugation using simple EDC-NHS conjugation chemistry. On the contrary, JPH203 possesses two primary amines; thus, impractical to be developed as a theranostic radiopharmaceutical using a similar conjugation method. In addition, the known

low solubility of JPH203 might hamper conjugation reactions [25,29].

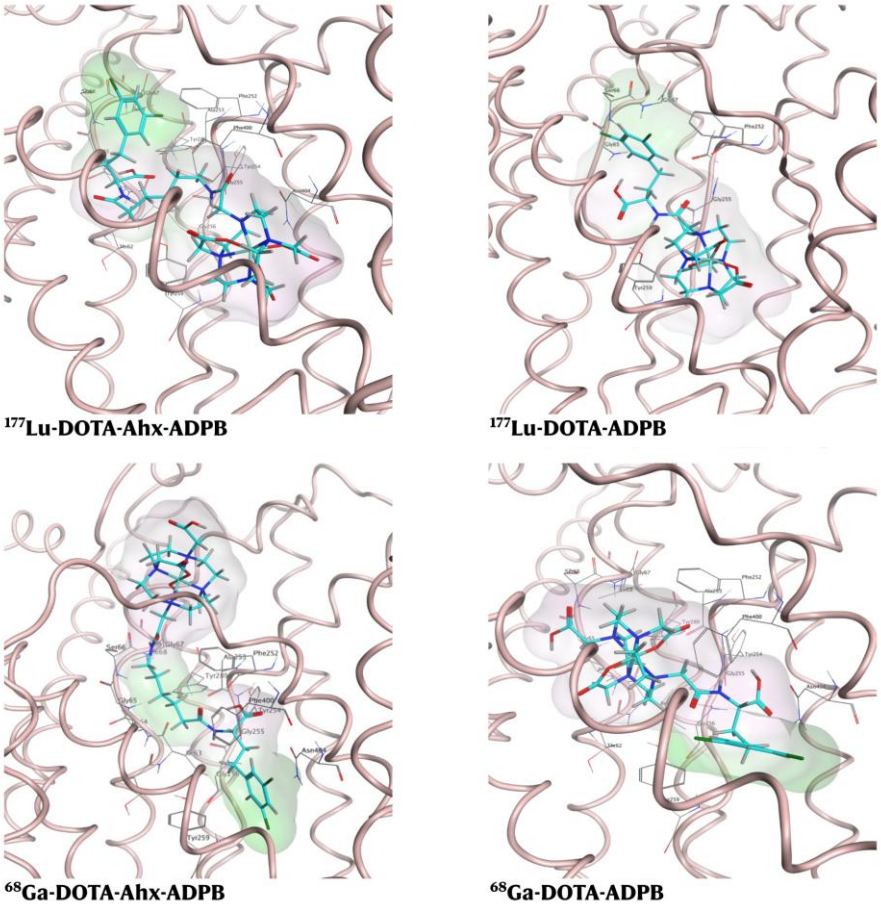

Figure 6. The 3D docking poses of ADPB-based theranostic radiopharmaceutical designs. Hydrophobic (*green shade*) and hydrophilic (*purple shade*) regions of the radiopharmaceutical designs

It is also important to note that the outer access to the LAT1 binding pocket is partially covered by a bulky extracellular domain 4F2hc subunit (**Figure 3**). Thus, a theranostic radiopharmaceutical conjugate targeting the LAT1 binding pocket must also be equipped with some degree of flexibility. Therefore, we added 6-aminohexanoic acid (Ahx) linker as a flexible methylene bridge between the chelating agent and the carrier molecule (**Figure 2**, **Supp. Data S2**). Ahx addition has proven useful in improving solubility and cell membrane permeability in various conjugates (from peptides to antibodies). More importantly, the presence of Ahx in the structures of the conjugate neither improves nor decreases biological activity but significantly improves the interaction with the molecular target [22]. The six carbon-length of Ahx also provided just enough distance between ADPB and chelator-metal complex to allow the overall conjugate to fit in the LAT1 binding pocket.

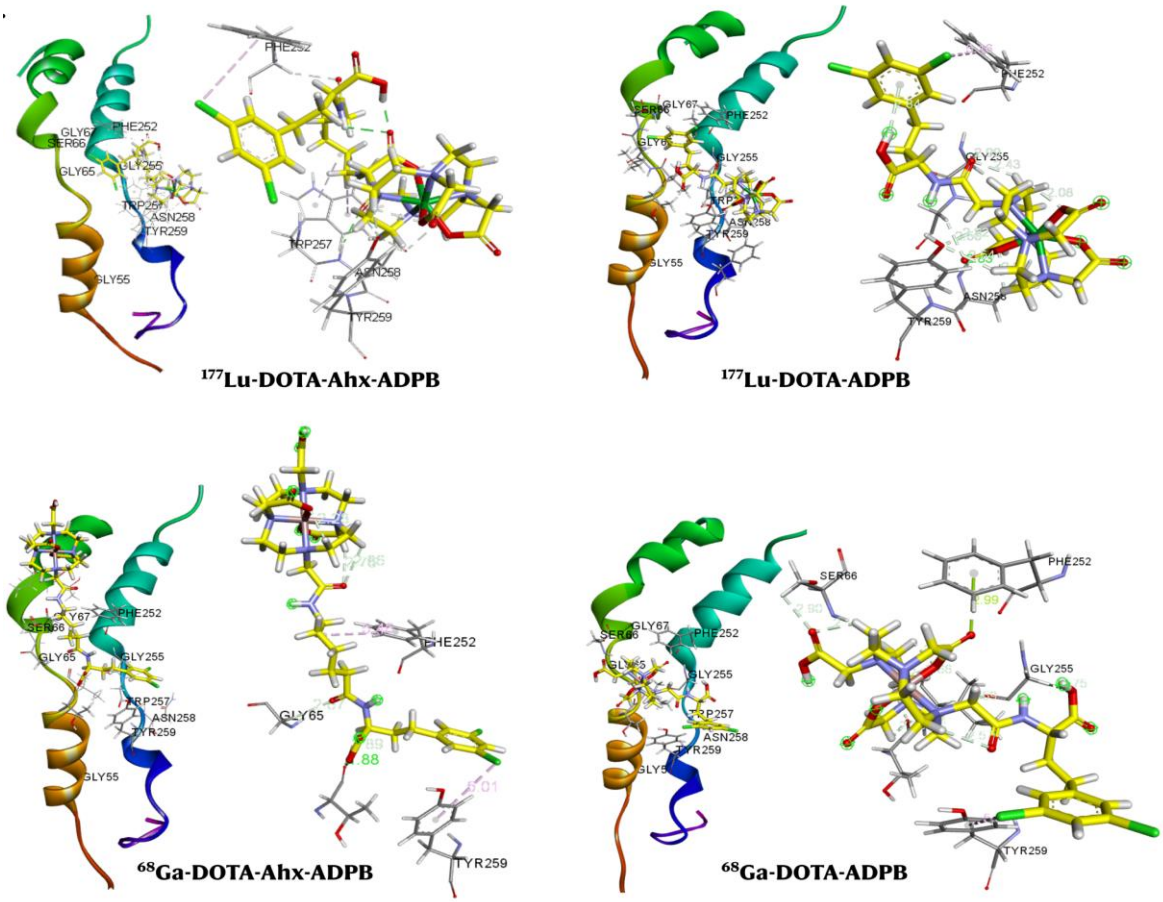

Figure 7. The 3D docking poses of ADPB-based theranostic radiopharmaceutical designs. Relative position against transmembrane helix 1 or TM1 (*light green* and *brown*) and transmembrane helix 6 or TM6 (*cyan and purple*) domains (***left***). Intermolecular interactions with key amino acid residues (***right***).

Eventually, we added DOTA, NOTA, and NODAGA as chelators to facilitate radiolabeling with theranostic radiometals. DOTA is regarded as an "industry standard" chelating agent due to its compatibility with useful radiometals such as ^{177}Lu, $^{86/90}$Y, ^{111}In, $^{44/47}$Sc, $^{212/213}$Bi, and $^{67/68}$Ga [23]. On the other hand, NOTA is considered a good chelator agent for the small ion Ga^{3+}, which fits well into its small cavity. NOTA is also promising for the clinical translation of radiopharmaceutical kits due to rapid radiolabeling at room temperature and mild pH to give a complex with high thermodynamics and excellent in vivo stability [30]. NODAGA (a NOTA-derivative) offers a similarly high-stability complex with ^{68}Ga but adds an extra negative charge via an additional carboxyl group [31]. NOTA and NODAGA were recently reported as potential BFCA for ^{99m}Tc/^{186}Re radiometal theranostic pair [32]; unfortunately, we could not successfully parameterize these metal prior to ligand preparation before docking simulations. Hence, we designed the theranostic radiopharmaceuticals using ^{177}Lu and ^{68}Ga, the most commonly used theranostic radionuclide pair. Even though ^{177}Lu also has diagnostic properties (□-ray emitter for SPECT camera), ^{68}Ga allows much better image resolution (with PET camera) [2].

In our molecular docking simulation, in vitro data of LAT1 inhibitors was used in trial docking 1) to generate a pharmacophore of LAT1 inhibition and 2) to finely select the refinement algorithm (scoring function) and build the final docking protocol for the main

study. Five scoring functions available in MOE employ different mathematical approaches to estimate the molecular interactions. Therefore, trial docking simulations were performed with each scoring function. The London dG algorithm was the scoring function that produced docking scores of LAT1 inhibitors highly correlated with their own *in vitro* predicted pIC_{50} values (**Supp. Data S6**). Thus, selecting the London dG algorithm for docking could be presumed as a closer mathematical approximation to the real LAT1 inhibition. The current approach has been proposed [33] and previously used to compare different molecular docking software and their unique algorithm [34].

Our docking simulation showed that LAT1 inhibitory potencies of ADPB-based theranostic radiopharmaceuticals enhanced when conjugated with particular radiometal-chelating agent complexes. Our most promising candidate compound, ^{177}Lu-DOTA-Ahx-ADPB (predicted pIC_{50} = 51.55), exhibited exceptionally high affinity to LAT1. Its similar version without linker addition, ^{177}Lu-DOTA-Ahx-ADPB, also demonstrated considerably high affinity (predicted pIC_{50} = 19.42). However, a similar result was neither observed in the case of ^{68}Ga-DOTA-Ahx-ADPB, ^{68}Ga-DOTA-ADPB, nor other ^{68}Ga-radiolabeled theranostic compounds. Therefore, we suspect that radiometal species may significantly impact the affinity. In light of this unexpected finding, we overlaid the 3D binding poses based on the same radiometal used. The overlaid image showed a striking difference in binding poses between ^{177}Lu-labeled and ^{68}Ga-labeled designs, almost irrespective of the carrier molecule (data not shown). Previous studies showed that radiometal ion has a marked influence on the affinity of the metal bioconjugates. However, such an effect is unpredictable [30]. Animal studies were performed to optimize which chelate for which radiometal is the most appropriate for the clinical translation of new theranostic drug candidates. For example, in case of DOTA-conjugated peptide SSTR antagonists, ^{68}Ga radiolabeling reduced the binding affinity, while ^{177}Lu radiolabeling retained the affinity similar to the native compound. Interestingly, ^{68}Ga radiolabeling improved the binding affinity of NODAGA-conjugated one compared to the native compound [35]. In other DOTA-peptide systems, e.g., pentixafor scaffold or bombesin-targeting peptides, the substitution of gallium by lutetium decreased the binding affinity by approximately an order of magnitude [36]. However, those phenomena were observed in larger conjugates (peptides) compared to ADPB-based theranostic radiopharmaceutical designs. Whether the opposite phenomenon applies in small molecule conjugates like ADPB-based compounds require further investigation.

The observation of intermolecular interaction showed that ^{177}Lu-DOTA-Ahx-ADPB and ^{177}Lu DOTA-ADPB have their ADPB moeity positioned on the upper part of the binding pocket and have strong bonds with residues in the unwound segment of transmembrane 6 (TM6) (**Figure 5**, **Figure 6**). Both have their chlorine atom on dichlorophenyl moeity interacting with the phenyl ring of proximal gating residue Phe252. Their chelate-radiometal complexes in the deeper part of the binding pocket possess strong hydrogen bonds with distal gating residues Asn258 and Tyr259. However, the higher affinity of ^{177}Lu-DOTA-Ahx-ADPB might be contributed by: 1) shorter intermolecular distance of hydrogen bond between Asn258 and ^{177}Lu-DOTA-Ahx-ADPB (2.21) than that of ^{177}Lu-DOTA-ADPB (2.83); and 2) additional carbon-hydrogen bond with Phe252. Previous studies showed that strong interaction with Phe252 is one of the key features of LAT1 inhibitors [18,19,21,25]. Any disturbance toward Phe252 may cause the LAT1 to lose its 100% transport capacity.The ADPB moeity of ^{68}Ga-

DOTA-Ahx-ADPB and ^{68}Ga-DOTA-ADPB are positioned distal within the binding pocket while making no significant interaction with TM6 residues, neither did their chelate-radiometal complex (**Figure 5**, **Figure 6**). According to Singh *et al.*, this pose is similar to halogenated ligands' most favored docking poses [19]. However, we did not observe any strong interaction between dichlorophenyl moieties of ^{68}Ga-DOTA-Ahx-ADPB nor ^{68}Ga-DOTA-ADPB with their surrounding key amino acid residues. Previous studies showed that the interaction of the amino acid moieties of LAT1 inhibitors with TM1 residues (Gly65, Ser66, and Gly67) contributes toward the total interaction free energies [18,19,21,25]. Unlike those amino acid-based small compounds, the amino acid moiety of ADPB in our design is being utilized for conjugation. Even though ^{68}Ga-DOTA-ADPB has strong hydrogen bonds with Gly65, Ser66, and Gly67, the total LAT1 inhibition potency is the lowest among four DOTA-conjugated ADPB-based designs. Thus, we suspect that interaction with TM1 is not as influential as interaction with amino acid residues of TM6 for LAT1 inhibitory potency of ADPB-based theranostic radiopharmaceutical designs. Even though both TM1 and TM6 undergo conformational change during the LAT1 transport cycle, TM6 tilts away more significantly from the binding site and provides steric occlusion via Phe252 side chain during LAT1 transport cycle. Hence TM6 (in particular, TM6a) is considered more responsible for LAT1 transport [20].

Regarding the whole structure shape, ^{177}Lu-DOTA-ADPB and ^{68}Ga-DOTA-ADPB are shorter and more globular than their counterpart version with Ahx linker. This conformation allows both designs to fill the binding pocket distal to the Phe252 side chain (**Figure 6a**). On the other hand, ^{177}Lu-DOTA-Ahx-ADPB and ^{68}Ga-DOTA-Ahx-ADPB behave differently with their linkers. ^{177}Lu-DOTA-Ahx-ADPB folded and flexibly fit within the binding pocket, while ^{68}Ga-DOTA-Ahx-ADPB stretched straight away beyond the upper part of the binding pocket. ^{68}Ga-DOTA-Ahx-ADPB did not exhibit a significant change of LAT1 inhibitory potency compared to the native ADPB (**Figure 4**, **Supp. Data S8**); however, it is interesting to note that ^{68}Ga-DOTA-ADPB whose conformation is fitted well within the binding pocket, failed to demonstrate a sufficient LAT1 inhibitory potency. This finding suggests the importance of the linker and its behavior when conjugating with a chelating agent and radiometal [22].

The hydrophobic effect of Ahx linker is more pronounced when the linker is straight (as in ^{68}Ga-DOTA-Ahx-ADPB, **Figure 6a**) than in folded state (as in ^{177}Lu-DOTA-Ahx-ADPB). In the classic LAT1 inhibition mode, a large hydrophobic side chain of the inhibitor occupies the large hydrophobic pocket surrounded by Gly255 and Trp257 in TM6 and Phe400, Trp405 and Val408 in TM10. However, despite the hydrophobic dichlorophenyl region of ^{68}Ga-DOTA-Ahx-ADPB and ^{68}Ga-DOTA-ADPB satisfying that pocket, these designs do not acquire considerable LAT1 inhibitory potency. The hydrophobic-hydrophilic moeity of LAT1 inhibitor has long been applied for small molecules (L-phenylalanine and other small substrates) [7]. Our findings suggest that such a moiety requirement might not apply to large conjugates. Ahx might have suitable length and hydrophobicity for LAT1 binding pocket; however, fine-tuning is highly recommended to obtain a better overall design, as observed in most development routes of theranostic radiopharmaceuticals. It is also important to consider the LAT1-selectivity of these LAT1-targeting radiopharmaceutical designs. Since the final structure is a complete departure from the amino acid scaffold, the proposed modifications to obtain LAT1 selectivity in previous LAT1 inhibitor discovery might not be applicable [7].

To our knowledge, this is the first study to propose a rational design of LAT1-targeting theranostic radiopharmaceutical. The LAT1 inhibitor, chemical scaffold, and the LAT1 crystal structure have been rationally selected for this particular purpose. The actual in vitro data was employed to refine the docking algorithm. However, this docking study is limited because it only describes the condition when the ligand is very close to the receptor's binding pocket. Even though molecular dynamic simulation may improve the estimation, while ADMET study may predict the in vivo pharmacokinetics, however, in vitro binding and in vivo studies in tumor xenografts will eventually provide more comprehensive data for further development stages. Synthesis and characterization of DOTA-Ahx-ADPB and DOTA-ADPB are ongoing.

Conclusions

In this study, we have developed a protocol for molecular docking simulation to evaluate the LAT1 inhibitory potency of LAT1 inhibitor-based theranostic radiopharmaceutical design comprised of the commercially available theranostic chemical scaffolds and a potent LAT1 inhibitor. The results of molecular docking simulations using MOE for various designed radiotheranostic complexes demonstrate the ability of ADPB-based and JPH203-based radiotheranostic conjugates with radionuclides ^{117}Lu and ^{68}Ga to inhibit LAT1 activity in cancer cells with good binding affinity and estimated pIC50 values. Furthermore, the intermolecular interactions between these radiopharmaceutical designs and the amino acid residues in the binding pocket could explain each design's strengths and weaknesses. In conclusion, our approach represents the first in silico evaluation of therapeutic radiopharmaceuticals targeting LAT1, providing a rational framework for predicting LAT1 binding and inhibition profiles. These results are expected to facilitate the rational development of next-generation LAT1-based therapeutic radiopharmaceuticals for various types of cancer, with improved selectivity, efficacy, and translational potential. The synthesis of the designed radiotheranostic compound, preclinical testing, and clinical testing are research stages that can be explored further to pave the way for the clinical use of ADPB-based and JPH203-based radiopharmaceuticals in patients.

Acknowledgement

This research (including APC) was supported and funded by Academic Leadership Grant from the Directorate of Research, Community Service, and Innovation of Universitas Padjadjaran on behalf of A.H.S.K., grant number 2203/UN6.3.1/PT.00/2022. The funders had no role in the design of the study; in the collection, analyses, or interpretation of data; in the writing of the manuscript, or in the decision to publish the results.

Author Contributions

Conceptualization, A.A. and H.A.H.; methodology, A.A., H.A.H., F.I.M., and B.S.A.S.; software, B.S.A.S.; validation, A.A. and F.I.M.; formal analysis, A.A. and F.I.M.; investigation, F.I.M., J.S., and A.A.E.; resources, H.A.H. and B.S.A.S.; data curation, A.A.; writing—original draft preparation, A.A.; writing—review and editing, A.A., F.I.M., H.A.H, and A.H.S.K.; visualization, A.A., F.I.M., and A.A.E; supervision, B.S.A.S.; project administration, A.H.S.K.; funding acquisition, A.H.S.K.. All authors have read and agreed to the published version of the manuscript.

Conflict of Interest

The authors declare no conflict of interest.

Ethical Standards

This article does not contain any studies involving human or animal subjects.

References

[1]. Sung H, Ferlay J, Siegel RL, Laversanne M, Soerjomataram I, Jemal A, et al. Global cancer statistics 2020: GLOBOCAN estimates of incidence and mortality worldwide for 36 cancers in 185 countries. *CA: a cancer journal for clinicians* **2021**; *71*:209-49. doi: DOI: 10.3322/caac.21660.

[2]. Roesch F, Martin M. Radiometal-theranostics: the first 20 years*. *Journal of Radioanalytical and Nuclear Chemistry* **2022**; DOI: 10.1007/s10967-022-08624-3.

[3]. Bodei L, Herrmann K, Schöder H, Scott AM, Lewis JS. Radiotheranostics in oncology: current challenges and emerging opportunities. *Nature Reviews Clinical Oncology* **2022**; DOI: 10.1038/s41571-022-00652-y.

[4]. Sollini M, Kirienko M, Gelardi F, Fiz F, Gozzi N, Chiti A. State-of-the-art of FAPI-PET imaging: a systematic review and meta-analysis. *European Journal of Nuclear Medicine and Molecular Imaging* **2021**; *48*:4396-414. doi: DOI: 10.1007/s00259-021-05475-0.

[5]. Buck AK, Haug A, Dreher N, Lambertini A, Higuchi T, Lapa C, et al. Imaging of C-X-C Motif Chemokine Receptor 4 Expression in 690 Patients with Solid or Hematologic Neoplasms Using ^{68}Ga-Pentixafor PET. *Journal of Nuclear Medicine* **2022**; *63*:1687. doi: DOI: 10.2967/jnumed.121.263693.

[6]. Fuchs BC, Bode BP. Amino acid transporters ASCT2 and LAT1 in cancer: partners in crime? *Seminars in Cancer Biology* **2005**; *15*:254-66. doi: DOI: 10.1016/j.semcancer.2005.04.005.

[7]. Kanai Y. Amino acid transporter LAT1 (SLC7A5) as a molecular target for cancer diagnosis and therapeutics. *Pharmacology & therapeutics* **2021**; 107964. doi: DOI: 10.1016/j.pharmthera.2021.10796

[8]. Broer S. Amino Acid Transporters as Targets for Cancer Therapy: Why, Where, When, and How. *International journal of molecular sciences* **2020**; *21*:DOI: 10.3390/ijms21176156.

[9]. Lopes C, Pereira C, Medeiros R. ASCT2 and LAT1 Contribution to the Hallmarks of Cancer: From a Molecular Perspective to Clinical Translation. *Cancers (Basel)* **2021**; *13*:DOI: 10.3390/cancers13020203.

[10]. Achmad A, Bhattarai A, Yudistiro R, Heryanto YD, Higuchi T, Tsushima Y. The diagnostic performance of ^{18}F-FAMT PET and ^{18}F-FDG PET for malignancy detection: a meta-analysis. *BMC Medical Imaging* **2017**; *17*:66. doi: DOI: 10.1186/s12880-017-0237-1.

[11]. Kim M, Achmad A, Higuchi T, Arisaka Y, Yokoo H, Yokoo S, et al. Effects of intratumoral inflammatory process on ^{18}F-FDG uptake: pathologic and comparative study with ^{18}F-fluoro-alpha-methyltyrosine PET/CT in oral squamous cell carcinoma. *Journal of Nuclear Medicine* **2015**; *56*:16-21. doi: DOI: 10.2967/jnumed.114.144014.

[12]. Hanaoka H, Ohshima Y, Yamaguchi A, Suzuki H, Ishioka NS, Higuchi T, et al. Novel ^{18}F-labeled α-methyl-phenylalanine derivative with high tumor accumulation and ideal pharmacokinetics for tumor-specific imaging. *Molecular Pharmaceutics* **2019**; *16*:3609-16. doi: DOI: 10.1021/acs.molpharmaceut.9b00446.

[13]. Nozaki S, Nakatani Y, Mawatari A, Hume WE, Wada Y, Ishii A, et al. First-in-human assessment of the novel LAT1 targeting PET probe ^{18}F-FIMP. *Biochemical and Biophysical Research Communications*

2022; *596*:83-87. doi: DOI: 10.1016/j.bbrc.2022.01.099.

[14]. Watabe T, Ikeda H, Nagamori S, Wiriyasermkul P, Tanaka Y, Naka S, et al. ^{18}F-FBPA as a tumor-specific probe of L-type amino acid transporter 1 (LAT1): a comparison study with ^{18}F-FDG and ^{11}C-Methionine PET. *European Journal of Nuclear Medicine and Molecular Imaging* **2017**; *44*:321-31. doi: DOI: 10.1007/s00259-016-3487-1.

[15]. Verhoeven J, Baguet T, Piron S, Pauwelyn G, Bouckaert C, Descamps B, et al. 2-[^{18}F]FELP, a novel LAT1-specific PET tracer, for the discrimination between glioblastoma, radiation necrosis and inflammation. *Nuclear Medicine and Biology* **2020**; *82-83*:9-16. doi: DOI: 10.1016/j.nucmedbio.2019.12.002.

[16]. Diagnostic PET/SPECT (Oncology PET) NKO-035 PET clinical research. 2022:

[17]. Watabe T, Naka S, Soeda F, Kamiya T, Sasaki H, Katayama D, et al. First in human dosimetry of ^{18}F-NKO-035: a new PET probe targeting L-type amino acid transporter 1 (LAT1). *Journal of Nuclear Medicine* **2020**; *61*:627. doi:

[18]. Singh N, Scalise M, Galluccio M, Wieder M, Seidel T, Langer T, et al. Discovery of potent inhibitors for the large neutral amino acid transporter 1 (LAT1) by structure-based methods. *International Journal of Molecular Sciences* **2019**; *20*:27. doi: DOI: 10.3390/ijms20010027.

[19]. Singh N, Villoutreix BO, Ecker GF. Rigorous sampling of docking poses unveils binding hypothesis for the halogenated ligands of L-type Amino acid Transporter 1 (LAT1). *Scientific Reports* **2019**; *9*:15061. doi: DOI: 10.1038/s41598-019-51455-8.

[20]. Floresta, G., Keeling, G., Memdouh, S., Meszaros, L., De Rosales, R., & Abbate, V. NHS-Functionalized THP Derivative for Efficient Synthesis of Kit-Based Precursors for 68Ga Labeled PET Probes. Biomedicines, **2021**, 9. https://doi.org/10.3390/biomedicines9040367.

[21]. Yan R, Li Y, Müller J, Zhang Y, Singer S, Xia L, et al. Mechanism of substrate transport and inhibition of the human LAT1-4F2hc amino acid transporter. *Cell Discovery* **2021**; *7*:16. doi: DOI: 10.1038/s41421-021-00247-4.

[22]. Markowska A, Markowski AR, Jarocka-Karpowicz I. The Importance of 6-Aminohexanoic Acid as a Hydrophobic, Flexible Structural Element. *International Journal of Molecular Sciences* **2021**; *22*:12122. doi: DOI: 10.3390/ijms222212122.

[23]. Holik HA, Ibrahim FM, Elaine AA, Putra BD, Achmad A, Kartamihardja AHS. The Chemical Scaffold of Theranostic Radiopharmaceuticals: Radionuclide, Bifunctional Chelator, and Pharmacokinetics Modifying Linker. *Molecules* **2022**; *27*:3062. doi: DOI: 10.3390/molecules27103062.

[24]. 24. Achmad A, Lestari S, Holik HA, Rahayu D, Bashari MH, Faried A, et al. Highly Specific L-Type Amino Acid Transporter 1 Inhibition by JPH203 as a Potential Pan-Cancer Treatment. *Processes* **2021**; *9*:1170. doi: DOI: 10.3390/pr9071170.

[25]. Yan R, Zhao X, Lei J, Zhou Q. Structure of the human LAT1–4F2hc heteromeric amino acid transporter complex. *Nature* **2019**; *568*:127-30. doi: DOI: 10.1038/s41586-019-1011-z.

[26]. Lu J-j, Li P, Yang Y, Wang L, Zhang Y, Zhu J-y, et al. Prognostic value of LAT-1 status in solid cancer: A systematic review and meta-analysis. *PLOS ONE* **2020**; *15*:e0233629. doi: DOI: 10.1371/journal.pone.0233629.

[27]. Zhang C, Xu J, Xue S, Ye J. Prognostic Value of L-Type Amino Acid Transporter 1 (LAT1) in Various Cancers: A Meta-

Analysis. *Molecular Diagnosis & Therapy* **2020**; *24*:523-36. doi: DOI: 10.1007/s40291-020-00470-x.

[28]. Kongpracha P, Nagamori S, Wiriyasermkul P, Tanaka Y, Kaneda K, Okuda S, et al. Structure-activity relationship of a novel series of inhibitors for cancer type transporter L-type amino acid transporter 1 (LAT1). *Journal of Pharmacological Sciences* **2017**; *133*:96-102. doi: DOI: 10.1016/j.jphs.2017.01.006.

[29]. Okano N, Naruge D, Kawai K, Kobayashi T, Nagashima F, Endou H, et al. First-in-human phase I study of JPH203, an L-type amino acid transporter 1 inhibitor, in patients with advanced solid tumors. *Investigative New Drugs* **2020**; DOI: 10.1007/s10637-020-00924-3.

[30]. Okarvi SM, Maecke HR. Chapter Eight - Radiometallo-Labeled Peptides in Tumor Diagnosis and Targeted Radionuclide Therapy. In: van Eldik R, Hubbard CD. Advances in Inorganic ChemistryAcademic Press; 2016:341-96.

[31]. Price EW, Orvig C. Matching chelators to radiometals for radiopharmaceuticals. *Chemical Society Reviews* **2014**; *43*:260-90. doi: DOI: 10.1039/c3cs60304k.

[32]. Makris G, Radford LL, Kuchuk M, Gallazzi F, Jurisson SS, Smith CJ, et al. NOTA and NODAGA [^{99m}Tc]Tc- and [^{186}Re]Re-Tricarbonyl Complexes: Radiochemistry and First Example of a [^{99m}Tc]Tc-NODAGA Somatostatin Receptor-Targeting Bioconjugate. *Bioconjugate Chemistry* **2018**; *29*:4040-49. doi: DOI: 10.1021/acs.bioconjchem.8b00670.

[33]. Sudarmanto BSA, Yuswanto A, Susidarti RA, Noegrohati S. Molecular Modeling of Human 3β-Hydroxysteroid Dehydrogenase Type 2: Combined Homology Modeling, Docking and QSAR Approach. *Jurnal Ilmu Kefarmasian Indonesia* **2017**; 7-16%V 15. doi:

[34]. 34. Azam SS, Abbasi SW. Molecular docking studies for the identification of novel melatoninergic inhibitors for acetylserotonin-O-methyltransferase using different docking routines. *Theoretical Biology and Medical Modelling* **2013**; *10*:63. doi: DOI: 10.1186/1742-4682-10-63.

[35]. Mansi R, Fani M. Design and development of the theranostic pair ^{177}Lu-OPS201/^{68}Ga-OPS202 for targeting somatostatin receptor expressing tumors. *Journal of Labelled Compounds and Radiopharmaceuticals* **2019**; *62*:635-45. doi: DOI: 10.1002/jlcr.3755.

[36]. Rousseau E, Lau J, Zhang Z, Zhang C, Kwon D, Uribe CF, et al. Comparison of biological properties of [^{177}Lu]Lu-ProBOMB1 and [^{177}Lu]Lu-NeoBOMB1 for GRPR targeting. *Journal of Labelled Compounds and Radiopharmaceuticals* **2020**; *63*:56-64. doi: DOI: 10.1002/jlcr.281